How Nucleus Mechanics and ECM Microstructure Influence the Invasion of Single Cells and Multicellular Aggregates

Noname manuscript No.
(will be inserted by the editor)

How Nucleus Mechanics and ECM Microstructure Influence the Invasion of Single Cells and Multicellular Aggregates.

Chiara Giverso · Alessandro Arduino · Luigi Preziosi

Received: date / Accepted: date

Abstract In order to move in a three-dimensional extracellular matrix, the nucleus of a cell must squeeze through the narrow spacing among the fibers and, by adhering to them, the cell needs to exert sufficiently strong traction forces. If the nucleus is too stiff, the spacing too narrow, or traction forces too weak, the cell is not able to penetrate the network. In this article we formulate a mathematical model based on an energetic approach, for cells entering cylindrical channels composed of extracellular matrix fibers. Treating the nucleus as an elastic body covered by an elastic membrane, the energetic balance leads to the definition of a necessary criterium for cells to pass through the regular network of fibers, depending on the traction forces exerted by the cells (or possibly passive stresses), the stretchability of the nuclear membrane, the stiffness of the nucleus, and the ratio of the pore size within the extracellular matrix with respect to the nucleus diameter. The obtained results highlight the importance of the interplay between mechanical properties of the cell and microscopic geometric characteristics of the extracellular matrix and give an estimate for a critical value of the pore size that represents the physical limit of migration and can be used in tumor growth models to predict their invasive potential in thick regions of ECM.

Keywords Cell migration · Cancer invasion · metastasis

PACS 87.17.Jj · 87.17.Rt

C. Giverso
Istituto Nazionale di Alta Matematica “F. Severi”, Città Universitaria
P.le Aldo Moro 5, 00185 Roma, Italy –
Department of Mathematical Sciences, Politecnico di Torino,
Corso Duca degli Abruzzi 24, 10129 Torino, Italy
E-mail: chiara.giverso@polito.it

A. Arduino
Department of Energy, Politecnico di Torino, Corso Duca degli Abruzzi 24, 10129 Torino, Italy
Istituto Nazionale di Ricerca Metrologica, Strada delle Cacce 91, 10135 Torino, Italy

L. Preziosi
Department of Mathematical Sciences, Politecnico di Torino,
Corso Duca degli Abruzzi 24, 10129 Torino, Italy

Mathematics Subject Classification (2000) 92B05 · 92C15 · 92C42 · 92C17

Highligth

In recent years, an increasing number of experimental works have been proposed to assess the cellular properties and functions involved in cell migration inside three-dimensional (3D) environments. In fact, when cells encounter narrow constrictions inside the 3D extracellular matrix (ECM), migration requires substantial cell deformation. In particular, biological experiments show that while the cytoplasm is very flexible and able to accommodate nearly any pore size, the cell nucleus (which is 5 to 10-fold stiffer than the cytoplasm) might be unable to squeeze through narrow pores, setting a critical pore size below which cell migration is abrogated. The rigidity of the cell nucleus, as demonstrated by a number of experimental works, is primarily derived from the chromatin mechanics inside the nucleus and the expression and assembly of lamins as part of the nuclear lamina. Thus, the description of 3D migration involves taking into account the nuclear mechanical characteristics, the ECM microstructure (that can be possibly modulated by the MMP secretion) and the ability of cells to actively generate the forces that propel the cell through constrained spaces.
On the basis of these biological observations, in this article we formulate a mathematical model based on an energetic approach, for cells entering cylindrical channels composed of extracellular matrix fibers. Treating the nucleus as an elastic body covered by an elastic membrane, the energetic balance leads to the definition of a necessary criterium for cells to pass through the regular network of fibers, depending on the stretchability of the nuclear membrane, the stiffness of the nucleus, the ECM pore size (compared to the nucleus diameter) and either the traction forces exerted by the cells or the passive stresses acting on the cell. We also show that the results obtained for a single cell migrating inside a cylindrical channel can be used into macroscopic tumor growth models to predict their invasive potential in thick regions of ECM.
The analytical and numerical results are discussed with respect to the biological data reported in literature for the parameters involved in the model and they reflect the biological findings that cell migratory capability depends upon size and deformability of the nucleus, due both to its solid interior and its elastic envelope, demonstrating the existence of a “physical limit” of migration.

1 Introduction

Acquiring an ability to move through the extracellular matrix and across membranes is a fundamental step in the invasion and spread of metastatic cancer cells [11, 20, 50, 54, 70]. Thus, in recent years an increasing number of experimental works, including Boyden chambers [58], Matrigel migration assays [58] and microfluidic platforms [20] have been proposed to assess the cellular properties and functions involved in cell

migration. While most of such experiments are performed on flat two-dimensional (2D) surfaces, cell motility in vivo typically takes place in a three-dimensional (3D) environment and biological tests on 3D migration [2, 5, 16, 18, 32, 47] indicate that in vivo cell motion can substantially differ to that on 2D substrates, since the geometric microscopic characteristics of the ECM may constitute a steric obstacle to cell motion [19, 32, 33, 70]. Indeed, in many cases the openings in 3D extracellular environments range from 2-30 μm in diameter [66] and hence might be substantially smaller than the cell diameter. When cells encounter these constrictions in the interstitial space, migration is supported by substantial deformation that allows cells to adapt their shape to the more rigid fibrillar network, and possibly by the localized production of proteolytic enzymes (e.g., Matrix Metalloproteinases, MMPs) that degrade matrix components and remove constricting fibers [15–18,33,38,47,51,53,69]. In particular, experiments [56, 57] show that whilst the cytoplasm is very flexible and able to accommodate nearly any pore size (including 1 μm^2 gaps in collagen gels and 0.8 μm^2 pores of polycarbonate membranes), the cell nucleus is 5 to 10-fold stiffer than the surrounding cytoplasm and, with a typical diameter of 3-10 μm, might be larger than the ECM fiber spacing [11]. During MMP-independent migration (i.e., when the proteolytic machinery is inhibited) and in spite of cell cytoplasm protrusions into the ECM trying to pull the nucleus inside, the stiff nucleus may be unable to squeeze through narrow pores, setting a critical pore size below which MMP-inhibited cells remain trapped [70]. This critical pore cross-section leads to the abrogation of migration and is estimated to be of the order of 10 % of the original nucleus cross-section (i.e., ≈ 7 μm^2 for tumor cells, ≈ 4 μm^2 for T cells and ≈ 2 μm^2 for neutrophils), irrespective of cell type and constitutive nuclear shape, and was defined as the "physical limit of migration" [70]. Residual migration below the critical pore size is strongly dependent on MMP-dependent ECM cleavage that partially degrades the fibres and enlarges matrix pore diameters to create a path for ECM invasion. Thus, alongside the size of network pores, which can be modulated by the MMP secretion, an ultimate rate-limiting physico-chemical determinants of cell migration [70] is the deformability of the nucleus in response to space constraints [11, 16, 18, 47]. This in turn depends on its composition and its mechano-coupling to the cytoskeleton and the surrounding environment [70].

Concerning the structure of the nucleus, it consists of dense genetic materials, called chromatin, surrounded by a lipid bilayer envelope with underlying networks of fibrous structural proteins, referred to as nuclear lamina [19, 20]. The nuclear lamina consists of a dense fibrillar network of type V-intermediate filaments, the lamins and lamin-associated proteins [70]. The rigidity, or deformability, of the cell nucleus, as demonstrated by a number of experimental works, is primarily derived from these two components: the level of chromatin compaction, which defines the physical compression limit [11, 14, 21, 38], and the expression and assembly of lamins as part of the nuclear lamina, which control nuclear shape and the pliability of the nucleus [6, 11, 14, 28, 34, 38, 39, 70]. In turn, lamin expression and the level of chromatin compaction are regulated by a number of mechanisms, with the ECM stiffness and pore size important contributors [38]. Indeed, nuclear lamina organization allows specific interactions with the cytoskeleton to the outside (through the Linker of Nucleoskeleton and Cytoskeleton, LINC), and with the intranuclear skeleton to

the inside (by direct and indirect associations) [33, 41]. Even chromatin, as part of the nucleoskeleton, is responsible for the mechanical coupling of the nucleus to the cytoskeleton to facilitate efficient cell migration and mechano-transduction [14, 21]. Hence, forces generated by the cytoskeleton, in response to the extracellular environment, can be transmitted to the nucleus and chromatin via physical links on the nuclear envelope and the lamin meshwork [43] and they can directly trigger changes in nuclear structures [33]. Thus, several experimental works have addressed the influence of the adhesive properties and active force generation of cells on their penetration of microchannels [25, 40, 51], drawing attention to the interplay between the mechanical properties of the cell nucleus, its connection to the cytoskeleton, as well as the geometrical properties of the environment [19, 32, 33, 70]. In particular, rather than the actual density of the ECM, it is the microscopic morphological characteristics of the extracellular environment that influence migration speed [70], since the same ECM fiber density can be achieved with either thinner fibers and smaller spacings among them on thicker fibers and larger spacings. Thus, modeling 3D migration involves taking into account the nuclear characteristics [16, 18, 47], the ECM microstructure [70] and the ability of cells to actively generate the forces that propel the cell through constrained spaces.

On the basis of these biological observations, Giverso et al. [22] identified a criterium of penetration based on an energetic argument. The criterium involves the ratio of quantities related to the adhesion forces exerted by the cells and either the stiffness of the nuclear membrane (in the case in which the nucleus is treated as an elastic membrane including a viscous liquid) or the Young's modulus of the nucleus (when it is treated as an elastic body). This ratio need to be compared to a function of the ratio of the ECM pore size with respect to the nucleus diameter, which then is in charge of describing the geometric characteristics of the ECM. In particular, it was demonstrated that if the size ratio is too restrictive then the cell cannot penetrate the ECM channel. Nevertheless, keeping the same geometrical characteristics, cell clones with higher traction abilities or softer nuclei might be able to invade the surrounding extracellular environment. Further, Giverso et al. [22] also found that modeling the nucleus only as an elastic membrane is not fully satisfactory, giving rise to certain paradoxes and concluded that it is more realistic to model the nucleus as an elastic solid.

However, as previously stated, the evidence that cells with softer perinuclear membranes are more motile in thick ECM [6, 11, 28, 34, 39, 70] suggests it is necessary to consider how the mechanical properties of both the nucleus and of the nuclear envelope determine cell mechanical properties and affect cell migration. Therefore, in the present paper we extend the preliminary work in [22] and propose a comprehensive mathematical model (see Section 2) based on an energetic approach, capable of describing the deformation of the initially spherical nucleus, treated as an elastic membrane surrounding an elastic solid nucleus, into an elongated deformed one, that can move inside a channel composed of ECM. While the ECM structure is highly complex in vivo, comprising of regions with strongly varying local densities [68], we consider the ECM as a structure of parallel cylindrical channels composed of fibers and bundles that provide directional guidance cues to cells. The resulting penetration criterium for a single cell entering an ECM channel is formulated and discussed in

Section 3. Then, based on the biological observation that the same phenomenon encountered for single cell migration in a 3D environment characterizes the invasion of multicellular spheroids in dense ECMs [70, 71], the results derived analytically using the energetic approach are extended in Section 4 to model the growth of cellular aggregates, following the work by Arduino et al. [1]. Applying the criterium deduced in this work to the growth of multicellular spheroids allows us to discriminate whether aggregates of tumor cells are able to invade the surrounding fibrous environment and when they can be segregated by thicker zones of ECM and porous membranes, as shown in [70].

2 Energy Balance Model

In order to penetrate a 3D extra-cellular matrix, cells need to deform and squeeze through the fiber network. In particular and as observed in the introduction, the nucleus (the stiffest organelle inside the cell) demands a substantial energy expenditure to deform sufficiently for penetration through smaller pores. This energetic cost is irrelevant when the cell is crawling on 2D substrata or in 3D networks with typical interfiber distances larger than the nuclear dimension, but increases considerably when the available spacing between the fibers is much smaller than the dimension of the nucleus. In this case nuclear deformation becomes a limiting factor to cell migration [71].

In the following evaluation, we assume that all the energy is spent deforming the elastic nuclear membrane and the internal solid nucleus, described as an elastic material, whereas the cytoplasm is treated as an inviscid liquid that can easily adapt to fit any channel size, so that the energetic contribution related to the deformation of it and the cell membrane can be neglected. The required energy might be provided both by the cell myosin-actin-focal adhesion machinery and by stress passively acting on the cell (i.e., fluid flow in microfluidic devices or the pressure of surrounding cells in multicellular aggregates). Hence, the paper develops under the requirement that for a cell to enter a channel, the energy needed to deform the nucleus and its membrane should be smaller than the work actively generated by the cell (i.e., through the integrin-mediated cytoskeletal contraction) and passively exerted on the cell (i.e., through stresses acting on the cell). Denoting respectively with $\mathcal{W}_{active}$ and $\mathcal{W}_{passive}$ these two contributions, the criterium for cell entrance inside a channel reads

$$\mathcal{W}_{active} + \mathcal{W}_{passive} \geq \mathcal{W}_{def} := \mathcal{W}^S_{def} + \mathcal{W}^V_{def}\,, \tag{1}$$

where we distinguished the energy related to membrane extension, $\mathcal{W}^S_{def}$, and the one related to bulk compression $\mathcal{W}^V_{def}$. Therefore, on the l.h.s. of eq. (1) we have the active and passive work, related to cell adhesion and stress, whereas on the r.h.s. we have the energy required to deform the cell. The cell can enter the channel only if the former is bigger than or, at worst, equal to the latter.

In the following, we will apply the criterium (1) to model the entrance of a single cell inside a cylindrical channel composed of ECM and we will explain in details how the different terms in inequality (1) have been derived. In particular, we observe that for the case of a single cell moving inside an extracellular environment in the

absence of fluid flows the deformation of the nucleus is mainly achieved by virtue of the integrin-mediated active forces generated by cytoskeleton contraction (see Section 2.2). Then, the criterium (1) can be detailed also for the motion of multicellular aggregates, in which case the passive contribution related to the growth of the aggregate cannot be neglected (see Section 4).

2.1 Deformation energy of the cell nucleus

Experimental evidences [65,70] suggest that when the cell is forced to cross channels of sterically limiting geometries, the central nucleus acquires an elongated shape oriented along the cell long-axis direction. Thus, we tackle the problem by considering that the initial spherical nucleus of radius R_n deforms into a prolate ellipsoidal nucleus, with minor semi-axes equal to the radius of the channel pore, R_p, preserving the total volume of the nucleus. In [22] it was shown that, while considering a cigar-like shape for the deformed nucleus leads to a more complicated analytical criterium, it yields quantitatively similar results.

As evident by the r.h.s. of eq. (1), the deformability of the nucleus mainly stems for two factors: the mechanical behavior of the chromatin inside the nucleus taken care in $\mathcal{W}^V_{def}$ and the expression and assembly of lamins as part of the nuclear envelope taken care in $\mathcal{W}^S_{def}$. Without going through the microscopic description of the mechanisms involved, which are still under study from an experimental point of view, the energy $\mathcal{W}^S_{def}$ can be approximated by the energy required to increase the surface area [13,24]

$$\mathcal{W}^S_{def} = \lambda(\Delta S)\Delta S^2\,, \tag{2}$$

where $\lambda(\Delta S)$ is the area stretch modulus and ΔS is the increase in the surface area of the cell as it passes from an initial spherical shape to its final conformation. In a first approximation $\lambda(\Delta S)$ can be considered constant, i.e., $\lambda(\Delta S) = \lambda_0$, but in general it can depend on the stretch experienced by the membrane. In particular, a maximum stretched area (S_{max}) might exist and in Section 3 both cases will be considered.
More refined relations for the membrane energy might be considered [29, 59–61]. Nevertheless, eq. (2) permits easier analytical computations and it has been shown to well represent cell behavior, at least within a certain range of deformations [13].
The increment in the surface area ΔS can be easily computed under the assumption that the volume of the deformed nucleus is equal to the volume of the initially spherical nucleus, V_{sphere}, so that

$$\Delta S = S_{ellips} - S_{sphere} = 2\pi R_p^2\left(1 + \frac{h_e}{R_p e}\sin^{-1}(e)\right) - 4\pi R_n^2 \tag{3}$$

where $e = \sqrt{1 - \dfrac{R_p^2}{h_e^2}}$, $h_e = \dfrac{R_n^3}{R_p^2}$ is the longer semi-axis of the prolate ellipsoidal nucleus (see Fig. 1(b)). By defining the dimensionless quantity $\tilde{R}_p = R_p/R_n$, eq. (3)

reduces to

$$\Delta S = 4\pi R_n^2 \left[\frac{1}{2}\tilde{R}_p^2 \left(1 + \frac{\sin^{-1}\left(\sqrt{1-\tilde{R}_p^6}\right)}{\tilde{R}_p^3\sqrt{1-\tilde{R}_p^6}} \right) - 1 \right] , \tag{4}$$

so that $\dfrac{\mathcal{W}_{def}^S}{(4\pi R_n^2)^2}$ is a function of $\tilde{R}_p$.

On the other hand, to compute the second term on the r.h.s. of eq. (1), we must calculate the deformation experienced by the solid bulk of the cell nucleus by assuming a proper constitutive equation, that represents the response of the material to deformations. While recent experiments [10, 12, 26] suggest a viscoelastic behavior of the cell nucleus, given the typical cell velocity range ($0.3 - 5\mu\mathrm{m/h}$ [68, 70], during MMP-independent migration) and the typical deformation and displacement required for nucleus entrance inside the channel (at least equal to the nucleus radius, i.e. $1.5 - 5\mu\mathrm{m}$ [11]), the time-scale required for cell entrance inside the channel will be orders of magnitude greater than typical nucleus relaxation times (estimated to be in the order of 20 seconds [26]). Hence the viscous contribution can be neglected and it is reasonable to approximate the nuclear mechanical behavior through a non-linear elastic constitutive law, such as the neo-Hookean one. Here, the stored elastic energy per unit volume is

$$\mathcal{W}^V = \frac{\mu}{2}\left[\mathrm{tr}(\overline{\mathbb{C}}) - 3\right] + \frac{k}{2}(J-1)^2 , \tag{5}$$

where $\mathbb{F}$ is the deformation gradient, $\overline{\mathbb{C}} = J^{-2/3}\mathbb{F}^T\mathbb{F}$, $J = \det(\mathbb{F})$, μ is the shear modulus and k is the bulk modulus of the nucleus. We consider here the nucleus as incompressible [37, 63], thus $J = 1$ and eq. (5) strongly simplifies. To compute the deformation gradient, we postulate that parallel planes perpendicular to the axis of the cylinder in the undeformed configuration are mapped onto parallel planes in the final deformed geometry, so that the deformation is simply uniaxial and

$$\mathbb{F} = \mathrm{diag}\left\{ \frac{R_p}{R_n}, \frac{R_p}{R_n}, \frac{R_n^2}{R_p^2} \right\} = \mathrm{diag}\left\{ \tilde{R}_p, \tilde{R}_p, \frac{1}{\tilde{R}_p^2} \right\} . \tag{6}$$

For the particular $\mathbb{F}$ considered, integrating the Neo-Hookean energy (5) over the total volume of the initial sphere, V_{sphere}, it is possible to compute the total energy required to deform the solid bulk of the nucleus, i.e.,

$$\mathcal{W}_{def}^V = \int_{V_{sphere}} \mathcal{W}^V dV = \frac{2}{3}\mu\pi R_n^3 \left(2\tilde{R}_p^2 + \frac{1}{\tilde{R}_p^4} - 3 \right) . \tag{7}$$

Finally, the elastic energy of deformation of the nucleus, considering the contributions of both the nuclear membrane and the solid bulk, is

$$\mathcal{W}_{def} = 16\pi^2\lambda(\Delta S)R_n^4\left[\frac{1}{2}\tilde{R}_p^2\left(1+\frac{\sin^{-1}\left(\sqrt{1-\tilde{R}_p^6}\right)}{\tilde{R}_p^3\sqrt{1-\tilde{R}_p^6}}\right)-1\right]^2 + \frac{2}{3}\mu\pi R_n^3\left(2\tilde{R}_p^2+\frac{1}{\tilde{R}_p^4}-3\right). \tag{8}$$

Thus, $\mathcal{W}_{def}$ depends on the mechanical properties of the solid nucleus, i.e., its shear modulus μ, its surface stretch modulus λ, and its size R_n as well as on the size of the ECM pore, R_p.

2.2 Cytoskeleton active work for a single cell

The nuclear deformation during cell migration through narrow openings inside the ECM requires important cytoskeletal forces that pull the nucleus through the fiber network [33]. In particular, migrating cells use both integrin mediated adhesion to the ECM and actomyosin-mediated contraction to propel the nucleus forward when dense ECM is transmigrated [70]. These forces, generated by the cytoskeleton contractility, can be transmitted to the nucleus via physical links on the nuclear envelope and the lamin meshwork [43], as outlined in the introduction. However, the effect of the active integrin-mediated traction forces on nuclear morphology and chromatin dynamics remains to be explored [43]. Without going into the details of the microscopic mechanism of force transmission, the criterium formulated in eq. (1) requires evaluation of the work exerted by the cytoskeleton machinery in order to have the cell completely inside the channel. This can be approximated by

$$\mathcal{W}_{active} = F^Z_{active}\Delta L\,, \tag{9}$$

where ΔL is the total displacement of the cell nucleus inside the channel, and F^Z_{active} is the resultant directed along the direction of motion (i.e., the Z-axis) of all forces exerted by the cytoskeleton. Referring to Fig.1, we considered that $\Delta L = L_n^{fin} - L_n^0$, where L_n^{fin} is the final length of the nucleus when it is totally inside the channel, whereas L_n^0 is the initial portion of the nucleus peeping into the channel without deforming. From elementary geometrical considerations, we have $L_n^{fin} = 2h_e$, where h_e is the longer semi-axis of the prolate ellipsoidal nucleus, as previously defined, and

$$L_n^0 = R_n - \sqrt{R_n^2 - R_p^2}\,, \tag{10}$$

so that

$$\Delta L = 2\frac{R_n^3}{R_p^2} - R_n + \sqrt{R_n^2 - R_p^2}\,. \tag{11}$$

To fulfil the description of the cytoskeleton work, a fundamental step is the definition of the active force generated by integrin-mediated cytoskeleton contraction.

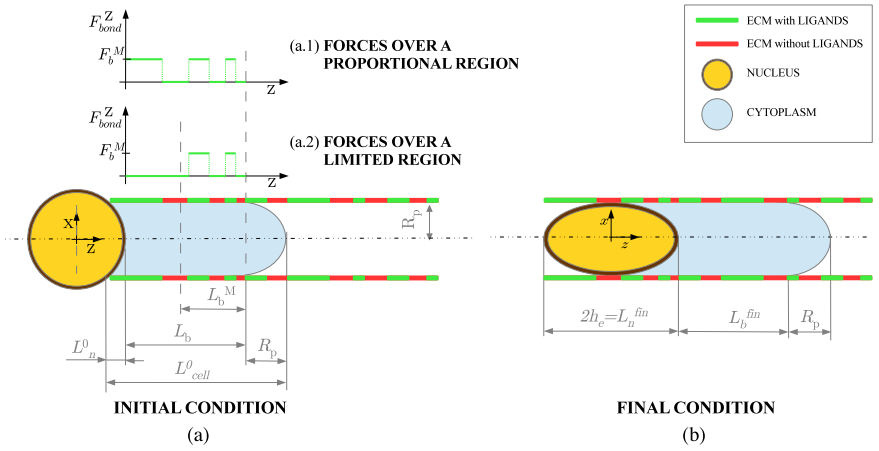

Fig. 1 Transverse section along the $X-Z$ plane of undeformed and deformed nucleus inside the channel. (a) Schematic representation of the different lengths introduced in the model (below) and of the assumptions used for the integrin-mediated active force (above). Considering as initial condition the case in which the cytoplasm is totally inside the channel, whereas the nucleus has experienced no deformation, we define by L^0_{cell} the length of the totally deformed cytoplasm of the cell and by L^0_n the length of the portion of the nucleus that can enter the channel without requiring nuclear deformation. The parameter L_b, which is the length of the deformed cytoplasm in front of the nucleus and in contact with the channel, can be obtained from eq. (14). When no restrictions are applied, bonds can form on all L_b ((a.1) *forces over a proportional region* case), depending on the ECM ligand sites fraction, α_{ECM} (green regions of the channel wall), and the density of adhesive bonds, so that the integrin-mediated active force acts on all $\alpha_{ECM} L_b$. In our model, we also consider the case in which the integrin-mediated active force might be generated only on a maximum portion of the cell membrane with length $\alpha_{ECM} L^M_b$ ((a.2) *forces over a limited region* case). (b) Schematic representation of the deformed nucleus inside the channel. Irrespective of the portion of the channel composed of ECM we consider that the deformed nucleus acquires the shape of a prolate ellipsoid, with minor axes equal to R_p and major axis equal to h_e. The length of the deformed cytoplasm in front of the nucleus and in contact with the channel in the final condition (i.e. when the nucleus is totally inside the channel) is equal to L^{fin}_b.

Activated integrins on the cell surface couple the cytoskeleton (in particular, the microfilaments) inside the cell to the ECM outside it, binding to ECM ligands (e.g., fibronectin, vitronectin, collagen and laminin). When this connection has been established, the cell may exert the active forces to propel itself. Different mechanisms have been proposed to describe how forces could be applied to the nucleus to move it through tight constrictions and it is challenging to distinguish between them by merely observing nuclear deformations [33]. In particular two major modes have been proposed: the cytoskeleton could exert forces from the cell front, pulling on the nucleus, or it could apply contractile forces from the rear of the nucleus, pushing and squeezing it through gaps in the ECM [33]. In particular, pulling forces could result from actin-myosin interactions that generate contractile forces between focal adhesion points and the anterior nuclear side, since, as shown in experiments [70], actomyosin-dependent force generation is fundamental in nonproteolytic cell migration. In the absence of experimental measurements of such forces, and without going into details on the complex actin-myosin machinery, we consider that the active force

can be thought as the resultant of all integrin-mediated forces generated through the contraction of the cytoskeleton. Thus, this active force can be modulated by the density of expressed and activated integrins, ρ_b, over the surface of contact between the cell and the ECM, and by the portion of the surface of contact composed by ECM ligands, α_{ECM}, i.e., the ratio of the channel surface for which the cell can actually bond with the ECM (see blue region on the surface wall section in Fig. 1).
While the density of expressed and activated integrins and the fraction of ECM composed by cell ligands generally depend on time [7, 9, 44], by focusing only on the time frame of nucleus squeezing in order to enter the channel, it is reasonable to assume ρ_b and α_{ECM} time independent. Indeed, during the time period considered for MMP-independent motion, the ligand-fraction α_{ECM} on the ECM channel wall is almost constant. Moreover, although the cell makes new attachments to the substrate at its front and simultaneously releases the older binding, detached integrins are subsequently taken back into the cell by endocytosis and transported to the cell front, where they are added to the surface. Hence, the total number of activated integrins on the cell surface can be taken as more or less independent over time. Under the assumption of time independent ρ_b and α_{ECM}, the total integrin-mediated active force is

$$\mathbf{F}_{active}(\mathbf{X}) = \int_{S_c} \rho_b(\mathbf{X})\alpha_{ECM}(\mathbf{X})\mathbf{F}_{bond}(\mathbf{X})dS\,, \tag{12}$$

where $\mathbf{X} = (X, Y, Z)$ and $\mathbf{F}_{bond}(\mathbf{X})$ is the force generated through cytoskeleton contraction, as a consequence of a single bond formation and S_c is the contact surface for which cell-ECM bonds might be expressed. Referring to Fig. 1 and assuming that the cytoplasm can easily penetrate inside the channel without any constriction, we can define

$$S_c = \left\{(X, Y, Z) : X^2 + Y^2 = R_p^2\,,\ \bar{Z}_{low}(t) < Z < \bar{Z}_{up}(t)\right\}\,. \tag{13}$$

Thus active forces will cause the translation of the cytosolic region (modeled as a cylinder with two spherical caps) and the deformation of the nucleus to advance inside the channels, with cross-section smaller than that of the nucleus. In the following we will consider the particular case in which the length for which integrin-mediated bonds could form, $\bar{Z}_{up}(t) - \bar{Z}_{low}(t)$, remains constant in time during cell deformation and we will call $L_b = \bar{Z}_{up}(0) - \bar{Z}_{low}(0)$ the length of contact. The length of contact is given by the portion of the cell in front of the nucleus in contact with the ECM channel (see Fig. 1)

$$L_b = L^0_{cell} - R_p - L^0_n\,, \tag{14}$$

L^0_n being defined by eq. (10) and L^0_{cell} being the length of the deformed cytoplasm of a cell of radius R_c that can freely enter inside the channel:

$$L^0_{cell} = R_p\left[\frac{4}{3}\frac{R_c^3 - R_n^3}{R_p^3} + \frac{1}{3} + \frac{1}{R_p^3}\left(L^0_n\right)^2\left(R_n - \frac{1}{3}L^0_n\right)\right]\,. \tag{15}$$

We remark that, rigorously speaking, the length of contact slightly changes during nucleus entrance into the channel. However, considering a cell of radius 15 μm [12]

with nuclear radius equal to 5 μm [12, 37], the discrepancy between L_b^{fin}, which is the length of contact in the final deformed configuration (see Fig. 1(b)), and L_b, the length of contact in the initial condition, is less than 1%. Therefore we can reasonably assume that L_b remain constant during the whole process, and take it equal to the initial length of contact.
In an almost homogeneous extracellular environment and considering a cylindrical channel, it is reasonable to assume axial symmetry and consider only the Z-component of that force, which is the one that makes the work required for the deformation. Thus, we have

$$F^Z_{active} = 2\pi R_p \int_0^{L_b} \rho_b(Z)\alpha_{ECM}(Z)F^Z_{bond}(Z)dZ\,, \tag{16}$$

i.e., the total active force is a function of the radius of the pore in the ECM, the density of bonds ρ_b, the surface fraction of the channel composed of ECM ligands, α_{ECM}, for which bonds can effectively form, and the integral of the single bond forces over the length of contact, L_b.
Furthermore, on the basis of experimental evidences [64] we consider that the length over which integrins bind ECM ligands is limited, typically to the apical portion of the moving cell. To do that we denote by L_b^M the maximal length of the region of contact (see Fig. 1(a)) and define this region through the indicator function

$$\chi_{L_b^M}(Z) = \begin{cases} 1 & \text{if} \quad (L_b - L_b^M)_+ < Z < L_b \\ 0 & \text{if} \quad 0 \le Z \le (L_b - L_b^M)_+ \vee Z \ge L_b \end{cases}$$

where $(\cdot)_+$ stands for the positive part of its argument. The above definition takes into account that for protrusions smaller than L_b^M adhesion might occur on the whole cytoplasmic membrane.
By considering the special case in which integrins and ECM ligands are homogeneous in space (a good approximation of in vitro conditions and reasonable for in vivo migration inside almost homogeneous environments) and taking as constant the integrin-mediated traction force over the region of contact (i.e., ρ_b, α_{ECM}, and $F^Z_{bond} = F_b^M$ are constant therein), eq. (16) simplifies to

$$F^Z_{active} = 2\pi R_p \rho_b \alpha_{ECM} F_b^M L_b^*\,, \tag{17}$$

where $L_b^* = \min\left\{L_b, L_b^M\right\}$. This relation prevents adhesive forces from dramatic growth as $R_p \to 0$ and is coherent with the fact that for very small pore radii the cell cannot extend its protrusion over excessively extended areas. A similar relation would be achieved if the region of contact is split into several disconnected intervals, where in this case $\chi_{L_b^M}$ is the sum of the intervals. Therefore, the present model can account also for cases in which activated integrins, interacting with ECM ligands on the surface of contact, cluster to form focal adhesion complexes. Focal adhesions contain integrin ligand, integrin molecule, and associate plaque proteins and provide sufficient binding sites to permit the formation of stable signaling complexes on the cell membrane. The density of integrins and ECM ligands inside these mature complexes and the force generated could reasonably be considered constant [7,67] so that,

accepting axial-symmetry, the model applies without further modification, under the convention that L_b^M is the total length of focal adhesive sites.
Finally, we observe that allowing $L_b^M \to \infty$ the region of contact corresponds to L_b and integrin-mediated forces are generated on a region of length $\alpha_{ECM} L_b$ proportional to the length of contact. Therefore in this latter case the region of contact is unbounded and grows to infinity for $R_p \to 0$. In the following we will refer to the case in which no limitations are set on the contact length as the *forces over a proportional region* case, whereas we will denote with *forces over a limited region* the case in which the length of the contact region is limited by L_b^M.

3 Application to Single Cell Migration

In the case of a single cell, whose motion is guided only by integrin-mediated traction forces, the proposed energy balance model states that a cell can enter inside the channel if

$$\mathcal{W}_{active} \geq \mathcal{W}_{def}\,,$$

with $\mathcal{W}_{active}$ given by (9) and $\mathcal{W}_{def}$ by eq. (8). In order to make explicit the above criterium, it is useful to define the dimensionless numbers

$$G_\mu := \frac{\rho_b \alpha_{ECM} F_b^M}{\mu} \quad \text{and} \quad \beta := \frac{\lambda R_n}{\mu}\,.$$

The former represents the ratio between adhesive-active properties (i.e., densities of bonds, surface ratio of ECM inside the channel, integrin-dependent traction force) and nuclear solid mechanical parameters (i.e., the shear modulus of the nucleus, treated as an incompressible Neo-Hookean material); the latter is a measure of the relative importance of surface stretchability versus bulk elasticity. The energetic inequality (1) then becomes

$$G_\mu \geq \beta \frac{8\pi \left[\dfrac{1}{2}\tilde{R}_p^2\left(1+\dfrac{\sin^{-1}(e)}{\tilde{R}_p^3 e}\right)-1\right]^2}{\tilde{R}_p \tilde{L}_b^* \Delta\tilde{L}} + \frac{1}{3}\frac{2\tilde{R}_p^2 + \dfrac{1}{\tilde{R}_p^4} - 3}{\tilde{R}_p \tilde{L}_b^* \Delta\tilde{L}} \tag{18}$$

where all quantities have been scaled with respect to the initial radius of the nucleus. For instance, $\tilde{R}_p = R_p/R_n$. In particular, $\tilde{L}_b^* = L_b^*/R_n = \min\left\{L_b/R_n, L_b^M/R_n\right\}$ is given by

$$\tilde{L}_b^* = \min\left\{\tilde{L}_b^M, \frac{4\tilde{R}_c^3 - 3\tilde{R}_p^2 - 2\tilde{R}_p^3 - 2 + 2(\tilde{R}_p^2-1)\sqrt{1-\tilde{R}_p^2}}{3\tilde{R}_p^2}\right\}.$$

As observed in the previous section, the case of forces over a proportional region is formally included by taking $L_b^M \to \infty$, so that eq. (18) takes into account the cases in which the region of contact is either limited or proportional to the entire cell

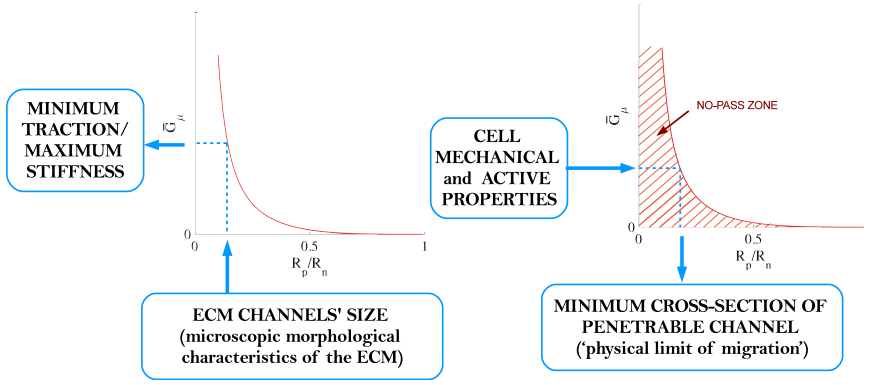

Fig. 2 Schematic representation of the biological interpretation of the relation between G_μ and $\tilde{R}_p$. The dashed region corresponds to the couple $(\tilde{R}_p, G_\mu)$ for which the cell cannot enter inside the ECM channel.

membrane area. Taking eqs. (10), (11), (14), (15) into account, it is possible to define the critical value of the characteristic number, $\overline{G}_\mu$

$$\overline{G}_\mu = \frac{8\pi\beta\left[\frac{1}{2}\tilde{R}_p^2\left(1+\frac{\sin^{-1}\left(\sqrt{1-\tilde{R}_p^6}\right)}{\tilde{R}_p^3\sqrt{1-\tilde{R}_p^6}}\right)-1\right]^2+\frac{1}{3}\left(2\tilde{R}_p^2+\frac{1}{\tilde{R}_p^4}-3\right)}{\tilde{R}_p\left[\frac{2}{\tilde{R}_p^2}-\left(1-\sqrt{1-\tilde{R}_p^2}\right)\right]\tilde{L}_b^*}, \tag{19}$$

below which a cell characterized by a given $G_\mu \leq \overline{G}_\mu$ cannot enter inside a channel of dimensionless radius $\tilde{R}_p$.

As illustrated in Fig. 2, given a cell of radius R_c with a nucleus of dimension R_n and nuclear mechanical properties characterized by a given $\beta_0 := \lambda_0 R_n/\mu$, for every diameter ratio $\tilde{R}_p$, it is possible to define the value of $\overline{G}_\mu$, such that for $G_\mu \leq \overline{G}_\mu$ the cell cannot enter inside a channel of radius $\tilde{R}_p R_n$. Conversely, knowing the density of expressed and activated integrins ρ_b on the contact surface S_c, the portion of the contact surface for which bonds can form α_{ECM}, the cytoskeletal traction force F_b^M generated after the formation of a single bond and, finally, the mechanical properties of the nucleus (i.e., its shear modulus μ and the ratio β_0), it is possible to derive the range of sizes of channel pores that can be penetrated by the cell.

Values of $\overline{G}_\mu$ are reported in Fig. 3, for different ratios of β_0, in the case in which

- no limitation is introduced for $\tilde{L}_b^*$ (left column), i.e., the extension of the surface of contact is the entire cell membrane (for $\alpha_{ECM} = 1$), or a fixed proportion of it ($\alpha_{ECM} < 1$);
- the extent of the region over which bonds can form is bounded (right column).

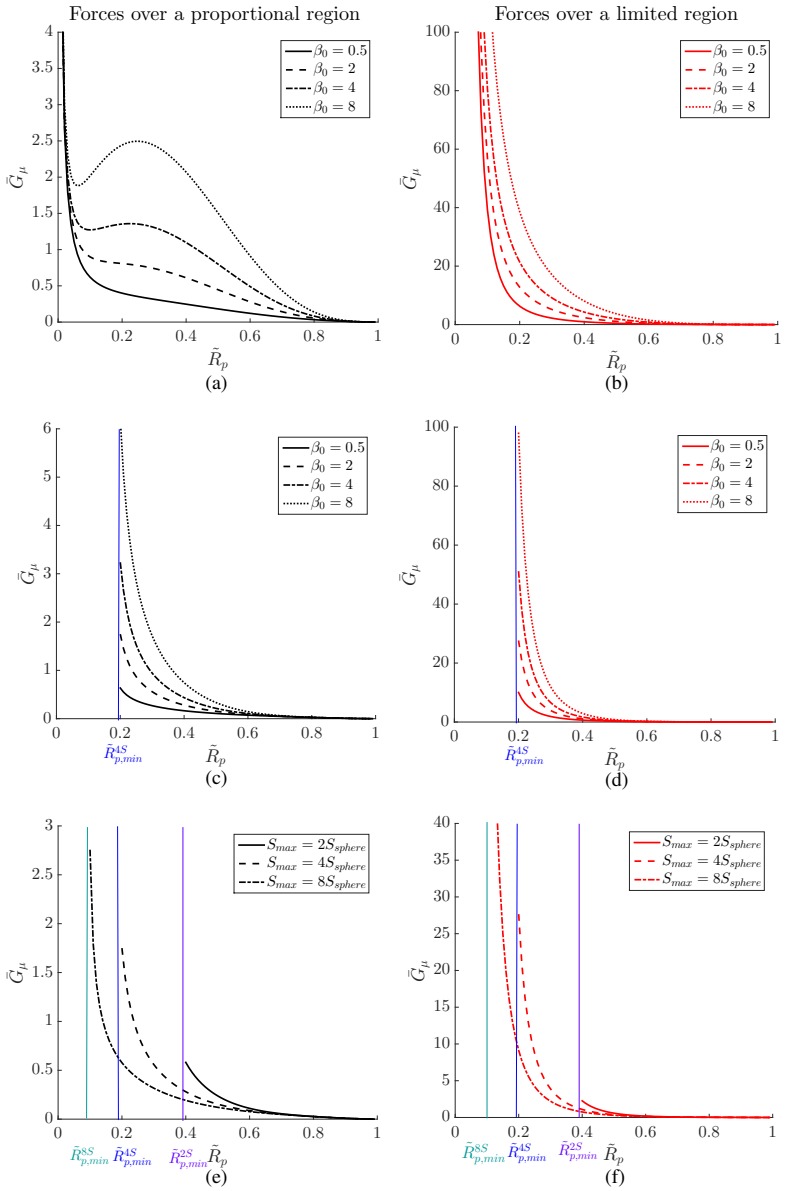

Fig. 3 Critical values of G_μ below which the cell cannot enter inside a channel of dimensionless radius $\tilde{R}_p$. The figure reports the plots of $\overline{G}_\mu$ when the region of contact is the entire cell surface or a fixed proportion of it (and thus it can potentially grow indefinitely) on the left column and when $\tilde{L}_b^*$ is bounded by $\tilde{L}_b^M = 5$ on the right column. In (a) and (b) $\lambda(\Delta S) = \lambda_0$ while in (c)-(f) $\lambda(\Delta S) = \lambda_0 \Delta S/(S_{max} - S)$. In (a)-(d) the value of $\beta_0 = \lambda_0 R_n/\mu$ is changed keeping μ fixed, whereas in (e)-(f) the value of S_{max} is changed keeping $\beta_0 = 2$. We denote with $\tilde{R}^{kS}_{p,min}$ $(k = 2, 4, 8)$, the minimum radius of the channel corresponding to the maximum extension of the nucleus membrane S_{max}, supposed equal to kS_{sphere}.

In particular, Figs. 3(a)-(b) report the values of $\overline{G}_\mu$ setting $\lambda(\Delta S) = \lambda_0$. We remark that since the proposed criterium takes into account the finiteness of the nuclear dimensions, the characteristic number $\overline{G}_\mu$ is defined only for $\tilde{R}_p \leq 1$. Indeed, when the nucleus is not required to deform in order to fit gaps in the ECM, the proposed model predicts that any cell can enter a channel with radius $R_p > R_n$, since we assumed that the cytoskeleton can freely enter inside channels of any dimension. Similarly, when $\tilde{R}_p \to 1$, the elastic energy required to deform the nucleus is very small, whereas the active work of integrin-dependent cytoskeletal forces is not null because the cytoskeleton extends inside the channel and thus, as shown in Fig. 3, $\overline{G}_\mu \to 0$, which means that the nucleus of the cell can be easily pulled inside the channel, even if the cell owns very low adhesive-active properties (i.e., low ρ_b, α_{ECM}, and F_b^M) or if the nucleus is very stiff (i.e., high μ and λ_0).
On the other hand, irrespective of the assumption made on $\tilde{L}_b$ and on the value of β_0, $\overline{G}_\mu \to \infty$ for $\tilde{R}_p \to 0$ (see Fig. 3(a)-(b)). For small radii, the behavior of $\overline{G}_\mu$ strongly depends on the assumption made on the extension of the region of contact and on the ratio $\lambda_0 R_n/\mu$. However, in the case in which no limitations on $\tilde{L}_b^*$ are introduced or equivalently $\tilde{L}_b^M = L_b^M/R_n \to \infty$ (see Fig. 3(a)) the graphs are not always monotonically decreasing. In fact, for a certain range of small pore sizes the advantage of a larger surface of contact overcome the drawback of requiring bigger deformation to squeeze the nucleus inside the narrow channel. In particular, looking at the two contributions on the energy of deformation, we have that $\mathcal{W}_{def}^S = \mathcal{O}\left(\tilde{R}_p^{-2}\right)$ and $\mathcal{W}_{def}^V = \mathcal{O}\left(\tilde{R}_p^{-4}\right)$ for $\tilde{R}_p \to 0$. On the other hand, looking at the active work of cytoskeletal forces and considering a region of contact that can grow without being bounded, $\mathcal{W}_{active} = \mathcal{O}\left(\tilde{R}_p^{-3}\right)$, being $\Delta\tilde{L} = \mathcal{O}\left(\tilde{R}_p^{-2}\right)$ and $\tilde{L}_b = \mathcal{O}\left(\tilde{R}_p^{-2}\right)$. Therefore, for $\lambda_0 R_n \gg \mu$ the contribution to $\overline{G}_\mu$ related to the elastic nuclear membrane dominates and, since the active work for small $\tilde{R}_p$ grows faster than the energy required to stretch the nuclear membrane, decreasing the channel pore size will allow cells that were trapped by a bigger channel to enter smaller ones, at least within a certain range (see region close to the relative maximum in the dotted and dash-dot lines in Fig. 3(a)). Eventually, as $\tilde{R}_p$ is substantially decreased further the cell can again not enter. This non-physical result is absent if it is assumed that bonds can form only on a portion of the cell up to a maximum length (see Fig. 3(b)), so that the active work of cytoskeletal forces cannot grow unrealistically. Indeed, in this case $\mathcal{W}_{active} = \mathcal{O}\left(\tilde{R}_p^{-1}\right)$, so that both the contribution related to the elastic membrane and the one due to the elastic solid nucleus allows $\overline{G}_\mu$ to grow to infinity for $\tilde{R}_p \to 0$ and the relation between $\overline{G}_\mu$ and $\tilde{R}_p$ is a bijection over all admissible ranges of pore radii.
Another mechanism that leads to the exclusion of the biologically unrealistic result described above consists of taking into account the existence of a maximum surface area for the nuclear membrane, S_{max}, above which the nuclear envelope cannot deformed any further. Hence the energy required to deform the elastic nuclear membrane grows indefinitely when $S \to S_{max}$. In Fig. 3 from (c) to (f) we report the

results obtained by setting

$$\lambda(\Delta S) = \lambda_0 \left(\frac{\Delta S}{S_{max} - S} \right)^n \quad \text{for } 0 \text{ and } \quad S \leq S_{max} \, .$$

In this case the relation between $\overline{G}_\mu$ and $\tilde{R}_p$ is a bijection in the region of definition of $\lambda(\Delta S)$, i.e. for $R_p > R_{p,min}$, with $R_{p,min}$ such that

$$2\pi R_{p,min}^2 \left(1 + \frac{R_n^3 \sin^{-1} \sqrt{1 - R_{p,min}^6 / R_n^6}}{R_{p,min}^3 \sqrt{1 - R_{p,min}^6 / R_n^6}} \right) = S_{max} \, ,$$

whatever assumption is made on the extension of the region of contact. For $\tilde{R}_p < \tilde{R}_{p,min}$ cells cannot penetrate the microchannel.
For all cases in which the relation between $\tilde{R}_p$ and $\overline{G}_\mu$ is a bijection, such as in Fig. 3 from (b) to (f), for every $\tilde{R}_p$ it is possible to uniquely define a $\overline{G}_\mu$, such that for $G_\mu < \overline{G}_\mu$ the nucleus cannot be pulled inside the channel. Conversely, knowing nuclear mechanical and active-adhesive properties, the minimum value of R_p that allows the nucleus of radius R_n to squeeze inside the channel can be determined.

Figures 3 from (a) to (f) also show the effect of increasing the surface stretch coefficient λ_0: cells characterized by a less stretchable membrane, in order to enter the same channel of a cell with lower λ_0, should increase their value of $\overline{G}_\mu$, acting on their adhesive-active abilities. This could occur by either increasing the number of adhesive bonds on the contact surface (ρ_b), or enlarging the portion of the contact area on which focal adhesion points can be formed (α_{ECM}), or, finally, raising the cytoskeletal traction force (F_b^M). At the same time, with $\overline{G}_\mu$ the ratio between adhesive-active characteristics and mechanical properties of the solid nucleus, these graphs show that in order to penetrate a channel with the same cross-section, cells with larger nuclear stiffness (greater μ and β_0 unchanged) should enhance their adhesive-active machinery, in order to maintain the same $\overline{G}_\mu$ even with increased stiffness of the solid nucleus. The effect of changing S_{max}, while keeping β_0 fixed is shown in Fig. 3(e)-(f). As expected, the minimum radius of the ECM channel that can be potentially penetrated by the cell increases for decreasing values of the threshold S_{max}.

In order to appreciate the effect of increasing solely the stiffness of the solid nuclear material (i.e., μ), it is better to report the energetic balance in terms of the newly defined characteristic number $G_\lambda = \dfrac{\rho_b \alpha_{ECM} F_b^M}{\lambda_0 R_n}$. If a cell increases the stiffness of its solid nucleus, corresponding to the curves in Fig. 4 for decreasing values of the ratio β_0, it might no longer be able to squeeze inside previously penetrable channels, unless it is able to enhance its active-adhesive abilities. As previously observed for G_μ, also in this case, the relation between $\tilde{R}_p$ and $\overline{G}_\lambda$ is a bijection only when the region of contact over which bonds can form is limited (Fig. 4(b)).

These analytical results reflect the biological finding highlighted by several experiments [3, 11, 51, 70, 71], that cell migratory capability depends upon size and deformability of the nucleus, due both to its solid interior (i.e., the chromatin) and

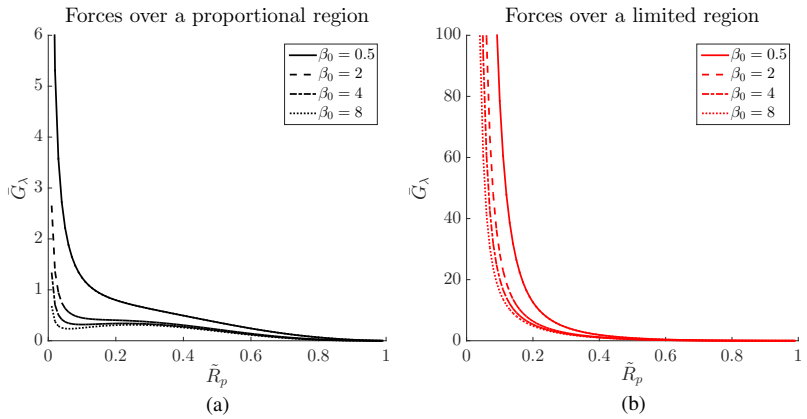

Fig. 4 Critical values of G_λ below which the cell cannot enter inside a channel of radius $\tilde{R}_p$, considering $\lambda(\Delta S) = \lambda_0$. The figure reports the plot of $\overline{G}_\lambda$ (a) in the case of forces over a proportional region and (b) in the case of forces over a limited region (with $\tilde{L}_b^M = 5$) for different value of β_0, keeping λ_0 fixed.

its elastic envelope (i.e., the nuclear lamina). In particular, large and stiff nuclei are much more resistant to large deformations and thus they impose a limitation during migration through narrow constrictions [70]. Even in the case in which the threshold on the maximum expansion of the nuclear membrane (S_{max}) is not introduced, since active-adhesive abilities cannot grow indefinitely, or equivalently the nucleus interior cannot become infinitely softer and its membrane infinitely stretchable, these results demonstrate the existence of a "physical limit" of migration, as outlined in some experimental works [52, 70].

Even though the analytical results are in qualitative agreement with biological experiments, a direct quantitative comparison between our predictions and the biological experiments is not straightforward. First, not all the data required by the mathematical model, even though measurable in principle, are reported in literature. Second, most of the works in the vast literature focus on the migration of cells on two-dimensional surfaces. However, we attempt to discuss the predictions of the proposed mathematical model with respect to biological data reported in literature and summarized in Table 1.

In particular, returning to the dimensional physical quantities, the density of integrins ρ_b in the region of adhesion has been estimated to be in the order of $700 - 1200$ integrins/μm^2 for mature adhesion and 365-600 integrins/μm^2 for regions with less strong adhesion (compared with 50-390 integrins/μm^2 in non-organized regions of the cell) [67]. The cytoskeleton force generated after the formation of a single bond can be estimated from [9], where a force of 5 nN per adhesive nanoisland of dimension 1 μm^2 is reported. Considering the integrin density reported in [67], we can estimate $F_b^M \approx 5 - 14$ pN. The portion of channel composed of ECM-binding sites depends on the amount of extracellular matrix forming the channel and on the density of ligands (such as fibronectin, vitronectin, collagen, and laminin) in the ECM. The percentage of these binding sites inside the ECM can significantly differ, ranging from $0.4 - 85\%$ [35, 49], and many experiments have been performed to evaluate the opti-

Table 1 Biologically meaningful ranges for the parameters of the microscopic model.

Parameter	Description	Values	Ref.
R_n	radius of the undeformed spherical nucleus	$1.5-5\,\mu\mathrm{m}$	[11, 12, 37]
R_c	radius of the undeformed spherical cell	$15.5\,\mu\mathrm{m}$	[12]
R_p	radius of the ECM pores	$0.5-5.5\,\mu\mathrm{m}$	[68, 70]
λ	nuclear membrane stretch modulus	$620\,\mathrm{MPa/m}$	[10]
μ	nucleus shear modulus	$0.07-10.7\,\mathrm{kPa}$	[12, 26, 27, 37]
ρ_b	density of integrins on the cell-ECM contact surface	$365-1200$ integrins $/\mu\mathrm{m}^2$	[67]
α_{ECM}	ligand density	$0.004-0.85$	[35, 49]
$\lvert\mathbf{F}_{bond}\rvert$	acto-myosin force	$\approx 5-14\,\mathrm{pN}$	[9, 67]

mal ligand density in order to favour cell migration, finding an optimal $\alpha_{ECM}\approx 0.5$ (corresponding to a particular ligand density of 1140 molecules/$\mu\mathrm{m}^2$) [9].
The mechanical properties of the nucleus have been estimated from the experimentally measured longitudinal displacements in one direction of a cell with $R_c = 15.5\,\mu\mathrm{m}$ and a nucleus with $R_n = 5\,\mu\mathrm{m}$ when a tensile load is applied, using finite element simulations [12]. The best fit between the numerical simulations and the experimental data leads to the estimation of $\mu = 10.7\,\mathrm{kPa}$ (elastic modulus of the nucleus $E = 32\,\mathrm{kPa}$), assuming an incompressible nucleus. On the other hand, using combined atomic force microscopy the nuclear Young's modulus for adherent fibrosarcoma cells on a glass substrate was measure to range between 0.2 and $2.5\,\mathrm{kPa}$ [37], leading to $\mu\approx 0.07-0.83\,\mathrm{kPa}$ (for an incompressible nucleus). This smaller value of nuclear elastic modulus is also consistent with the value derived for chemically isolated nuclei of articular chondrocytes using micropipette aspiration [26], that was reported to be of the order of $1\,\mathrm{kPa}$ ($\mu = 0.33\,\mathrm{kPa}$). Intermediate values of nuclear stiffness can be found in [27], where they reported an elastic modulus of $5.67-8.4\,\mathrm{kPa}$ ($\mu = 1.89-2.8\,\mathrm{kPa}$) for metastatic bladder cancer cell and a Young's modulus of $9.29\mathrm{kPa}$ ($\mu = 3.1\,\mathrm{kPa}$) for isolated nuclei of fibroblast-like valve interstitial cell. Furthermore Liu et al. [27] measure a higher Young's modulus of $26.54\,\mathrm{kPa}$ ($\mu = 8.85\,\mathrm{kPa}$) for nuclei within intact fibroblast-like valve interstitial cells on soft substrates, comparable with the value reported in [12] for intact cells.
The nuclear membrane stretch modulus can be estimated from the micropipette aspiration experiment performed in [10] on swollen and unswollen nuclear envelopes, that leads to an averaged dilation modulus $K\approx 390\,\mathrm{mN/m}$. Considering the homogeneous conditions under which the proposed model has been derived, it is possible to compute $\lambda = K/(2S_0) = 620\,\mathrm{MPa/m}$ for a nucleus of radius $5\,\mu\mathrm{m}$.
Therefore, using the parameters summarized in Table 1, for a cell characterized by $R_n = 5\mu\mathrm{m}$ [12, 37], it is possible to estimate $\beta_0\approx 0.29-44.3$ and, for an optimal ligand fraction of the ECM (i.e $\alpha_{ECM} = 0.5$), we have $\overline{G}_\mu = 0.085-120$, which are in good agreement with the range of values predicted by our mathematical model. In particular, the maximal deformation limit of 10% of the initial undeformed nuclear cross-section reported in [37], considering an averaged elastic modulus for the cell nucleus, corresponds to a $\overline{G}_\mu = 3.75$ considering forces over a limited region (with

$\tilde{L}_b^M = 5$), which is in the biological range, whereas it leads to $\overline{G}_\mu = 0.05$ in the case of forces over a proportional region, which is sligthly below the physiological range. Thus a bounded model seems more representative of the real biological conditions. However we remark that this "physical limit" for cell migration has been derived for nuclei experiencing hourglass deformation, whereas for ellipsoidal deformation the maximal deformation limit could be larger.

4 Application to Multicellular Aggregates

The same mechanisms outlined for the case of single cell migration inside an ECM channel also characterize and limit the invasion of multicellular aggregates while growing in dense ECMs [70]. Indeed, the cells at the border of the cellular spheroid try to penetrate the surrounding fiber network, but, whereas their cytoplasm is able to extend into the channels of the ECM as observed for single cells, their nuclei might remain trapped at the border of the aggregate, depending on the geometrical (in particular, the typical pore size of the extracellular network) and mechanical properties of the cells (especially, the stiffness of the cells' nuclei) [70].

In particular, when the spheroid is immersed in an ECM network with a pore size that is not sterically restrictive, the cells at the outer border of the spheroid can invade the surrounding collagenous environment. On the other hand, when the pore size in the collagen network is too small (with respect to the nuclear dimension) and the cells in the multicellular aggregate cannot secrete MMPs, the cells cannot invade the surrounding tissue, since their nuclei remain trapped at the border of the spheroid, even though their cytoplasms tend to protrude into the network.

Starting from this experimental observation, it is clear that the potential segregation of spheroids cannot be accounted for by standard continuum macroscopic models that treat the multicellular aggregate as a simple fluid (viscous or inviscid) and relate the velocity of cells to cell pressure through a sort of Darcy's law with a permeability coefficient that is usually constant or weakly depending on the ECM volume fraction [42, 48, 64], because any cell pressure would lead to penetration of the surrounding porous structures.

Therefore, bearing in mind the analytical results presented in the previous section, we extend the multiphase model proposed in [1] to describe the macroscopic migration and segregation by thick porous structures of multicellular aggregates, taking into account the limitations imposed by the nuclear envelope and its solid interior material.

The cell aggregate is modeled as a mixture of cells, ECM components and interstitial fluid, whose volume fractions are denoted respectively by ϕ_c, ϕ_m, and ϕ_ℓ. In particular, we assume that the cellular population lives in a rigid ECM and behaves like a simple elastic fluid with Cauchy stress tensor

$$\mathbb{T}_c(\psi) = -\Sigma(\psi)\,\mathbb{I} = E\frac{1-\phi_n}{1-\psi}(\psi-\phi_n)_+\,\mathbb{I}\,, \tag{20}$$

where $\psi := \phi_c + \phi_m$ denotes the solid volume ratio, E is analogous to the Young's modulus for low compression, ϕ_n is the highest volume ratio below which cells experience no compression, and $\mathbb{I}$ is the identity tensor. In principle, one should consider,

beyond this passive contribution to the stress tensor, also an active part that relates to the traction forces that the cells are able to exert by adhering to the ECM and contracting the acto-myosin machinery inside their cytoplasm. However, whereas in the case of single-cell migration the active contribution is generally more significant than the passive pressure exerted by fluid flow, in the case of growing multicellular aggregates we assume that passive forces lead the evolution of the system.
Consistently, it is assumed that the growth of the multicellular aggregate is merely limited by cell-cell compression (i.e., contact inhibition of growth), with nutrients being abundant everywhere. Thus, the cell supply term reads [8]

$$\Gamma_c = \left[\gamma_c \mathcal{H}_\varepsilon(\psi_0 - \psi) - \delta_c\right] \phi_c \,, \tag{21}$$

where ψ_0 is the threshold value of the solid volume ratio that triggers contact inhibition, γ_c is the duplication rate of cells, δ_c is the apoptotic rate and $\mathcal{H}_\varepsilon$ is a continuous mollificator of the Heaviside step function, namely

$$\mathcal{H}_\varepsilon(\psi_0 - \psi) = \begin{cases} 0\,, & \text{if } \psi \geq \psi_0\,; \\ (\psi_0 - \psi)/\varepsilon\,, & \text{if } \psi_0 - \varepsilon \leq \psi < \psi_0\,; \\ 1\,, & \text{if } \psi < \psi_0 - \varepsilon\,. \end{cases} \tag{22}$$

In addition, as considered for the single cell, in order to simulate the growth of a multicellular spheroid during MMP-independent migration, the production of matrix degrading enzymes will not be considered. Following [1, 23], it is possible to show that the mass and momentum balance describing the evolution of the mixture and its constituents may be reduced to the single equation

$$\frac{\partial \phi_c}{\partial t} + \nabla \cdot \left(\phi_c \Sigma'(\psi) \mathbb{M} \nabla \psi\right) = \Gamma_c \,, \tag{23}$$

where $\mathbb{M}$ is the motility tensor. From the experimental study reported in [70], $\mathbb{M}$ cannot be constant but should depend on the pore area of the ECM, A_m, and on the force exerted on the cells, that permits the definition of a threshold pore cross-section A_0 below which the migration of cells is forbidden, as described in the previous sections. Referring to [1], the motility tensor can be written in the isotropic case as

$$\mathbb{M} = M\, \mathbb{I} = \alpha \frac{[A_m - A_0]_+}{\left(1 + \dfrac{A_m - A_0}{A_1}\right)^n} \mathbb{I}\,, \tag{24}$$

that reduces to the linear motility observed in [70] when $n = 0$ or $A_m \to A_0$. Since, to the best of our knowledge, no experiments have been performed that help in evaluating neither A_1 (which is related to the existence of an optimal pore cross-section for which a maximal cell motility is observed) nor n, in the following we assume $n = 0$. The dimension of the pore area A_m for a given volume ratio of ECM ϕ_m can be analytically estimated by assuming that the peptide fibers that constitutes the ECM are locally disposed as a cartesian crystal lattice. This assumption leads to the definition of $A_m(\phi_m)$ by formally inverting the relation [1]

$$\phi_m = \frac{3\sqrt{A_m/A_f} + 1}{\left(\sqrt{A_m/A_f} + 1\right)^3}\,, \tag{25}$$

where A_f is the area of the cross-section of a fiber bundle, that is a collection of up to $50-100$ fibrils [4].

The threshold value of A_0 can be obtained by writing down the energetic balance

$$\mathcal{W}_{passive} \geq \mathcal{W}_{def}\,, \tag{26}$$

where with respect to (1), the contribution of active forces has been neglected. The reasoning here is that for multicellular aggregates it is reasonable to assume that the force actively exerted by the single cell, attaching and pulling on the ECM fibers, is negligible with respect to the force passively experienced by the cell due to the pressure of all other cells growing in the spheroid.
Despite an assumption of isotropic disposition of the ECM fiber bundle, instead of a tubular organization as in Section 2, we still consider that the deformed nucleus acquires the shape of a prolate ellipsoid, as in the case of a single cell, so that the energy required to deform the nucleus of the cells, $\mathcal{W}_{def}$, is given by (8). On the other hand, the passive work $\mathcal{W}_{passive}$ can be related to the hydrostatic part of the stress by

$$\mathcal{W}_{passive} = \frac{1}{3}|\mathrm{tr}\mathbb{T}_c|\pi R_p^2 \Delta L = \Sigma(\psi) A_0 \Delta L\,. \tag{27}$$

Consequently, the energetic balance leads to the definition of the characteristic number $G_{passive} = \Sigma(\psi)/\mu$ and to the definition of its critical value

$$\overline{G}_{passive} = \frac{16\pi\beta\left[\dfrac{\tilde{R}_p^2}{2}\left(1+\dfrac{\sin^{-1}\left(\sqrt{1-\tilde{R}_p^6}\right)}{\tilde{R}_p^3\sqrt{1-\tilde{R}_p^6}}\right)-1\right]^2+\dfrac{2}{3}\left(2\tilde{R}_p^2+\tilde{R}_p^{-4}-3\right)}{\tilde{R}_p^2\left(2\tilde{R}_p^{-2}-1+\sqrt{1-\tilde{R}_p^2}\right)}\,. \tag{28}$$

Calling $g(\tilde{R}_p)$ the right-hand-side of eq. (28), the threshold value $A_0 = \pi(R_n\tilde{R}_p)^2$ can be evaluated by formally inverting the relationship $g(\tilde{R}_p) = G_{passive}$, namely

$$A_0 = \pi\left(R_n g^{-1}\left(G_{passive}\right)\right)^2\,. \tag{29}$$

Thus, the threshold value A_0 depends on nucleus stiffness and dimension and on the stress exerted on the cell, or equivalently on the solid volume ratio ψ. It is worth noting that, whereas the first dependencies are related to the cell nature, which in our simulations will be described by constant parameters, the last one evolves dynamically with the system. For this reason we write $A_0 = A_0(\psi)$.

By collecting all the proposed modeling assumptions, and by scaling times with $1/\gamma_c$, lengths with $\sqrt{\alpha A_n E/\gamma_c}$, where $A_n = \pi R_n^2$ is the area of the maximum circle of cell nucleus at rest, and stresses with E, eq. (23) can be written in dimensionless form as

$$\frac{\partial\phi_c}{\partial\tilde{t}} - \tilde{\nabla}\cdot\left[\phi_c\left(\tilde{A}(\phi_m)-\tilde{A}_0(\psi)\right)_+\tilde{\nabla}\tilde{\Sigma}(\psi)\right) = \left[\mathcal{H}_\varepsilon(\psi_0-\psi)-\tilde{\delta}_c\right]\phi_c\,, \tag{30}$$

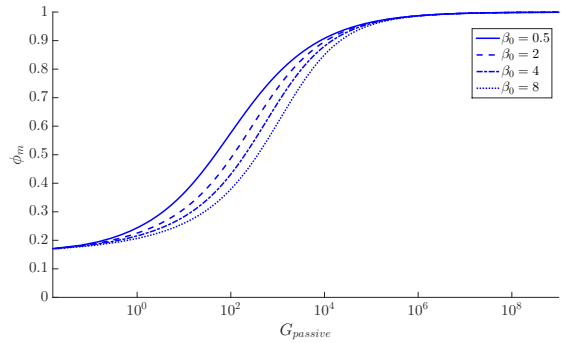

Fig. 5 To each characteristic number $G_{passive}$ is associated the corresponding maximum volume ratio of ECM that can be crossed for $\tilde{A}_f = 0.09$ and $\beta_0 = 0.5$, 2, 4, and 8.

where the tilde denotes the dimensionless quantities and where

$$\tilde{A}(\phi_m) = A(\phi_m)/A_n\,, \qquad \tilde{A}_0(\psi) = A_0(\psi)/A_n = g^{-1}(\tilde{E}\tilde{\Sigma}(\psi))^2\,.$$

Thus, the problem only depends on the dimensionless parameters $\tilde{\delta}_c = \delta_c/\gamma_c$, $\tilde{E} = E/\mu$ and $\tilde{A}_f = A_f/A_n$ in addition to the already non-dimensional quantities β, ψ_0, ϕ_n and ε.

It is interesting to combine the functions $\tilde{A}_m(\phi_m)$ and $\tilde{A}_0(\psi)$ in order to find a relation that for any given characteristic number $G_{passive}$ associates the maximum volume fraction of ECM that can be crossed by the cell aggregate. For the non-dimensional parameter $\tilde{A}_f = 0.09$, in Fig. 5 this relation is reported for a certain value of β_0. As one would expect, when β_0 increases, namely the rigidity of the nuclear lamina increases with respect to the rigidity of the solid nuclear material, the maximum density of ECM that can be crossed by the cellular aggregate with fixed characteristic number decreases.

Figure 6 shows the results obtained by solving eq. (30) on a one-dimensional domain, $\Omega = [0, 1]$, divided into two regions: one region, denoted by Ω_m^+, characterized by a higher density of ECM, ϕ_m^+, and the other with a lower density, ϕ_m^-. Specifically

$$\phi_m(\mathbf{x}) = \begin{cases} \phi_m^+\,, \text{ if } \mathbf{x} \in \Omega_m^+ \\ \\ \phi_m^-\,, \text{ otherwise} \end{cases} \tag{31}$$

Equation (30) is solved by the finite volume numerical method. It has been chosen due to its capability in handling the degenerate nature of the equation, which can be in each point parabolic or hyperbolic depending on the solution itself. In addition, the finite volume method guarantees that the approximate solution correctly handles mass balance. The results are reported for different values of the non-dimensional parameters β_0 and $\tilde{E}$. When $\tilde{E}$ is the lowest, either because the cell phase has the lowest Young's modulus E or because the nucleus rigidity μ is the highest, the cellular aggregate cannot move toward the region with higher density of ECM, where the pores are narrower, and so it remains segregated for all considered values of β_0,

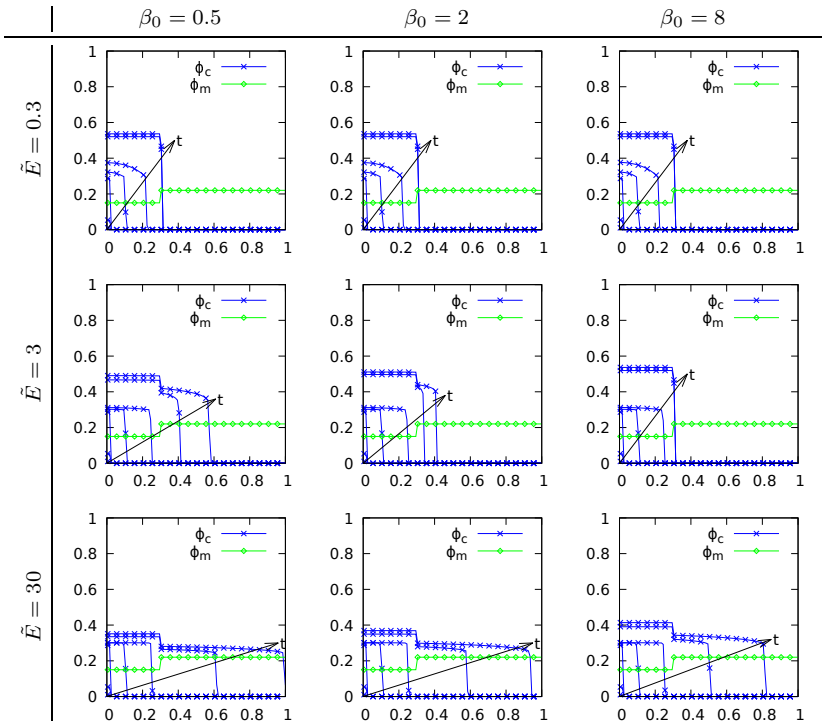

Fig. 6 Solutions of eq. (30) for different combinations of $\tilde{E}$ and β_0 on a one-dimensional domain with ECM distributed according to eq. (31) where $\Omega_m^+ = [0.3, 1]$, $\phi_m^+ = 0.22$ and $\phi_m^- = 0.15$. The parameters are assumed to be $\tilde{\delta}_c = 1/8$, $\tilde{A}_f = 0.09$, $\psi_0 = 0.7$, $\phi_n = 0.45$ and $\varepsilon = 0.1$. Each plot contains the solution at the dimensionless instants $\tilde{t} = 0$, 2, 4, 6, 7, 8, and 8.55.

independently on how elastic is the nuclear membrane. In the case $\tilde{E} = 3$, the cell aggregate is segregated or not accordingly to β_0. Precisely, when the nuclear envelope is more elastic ($\beta_0 = 0.5, 2$) the aggregate can invade the region with thicker ECM, whereas this is not possible in case of a more rigid envelope ($\beta_0 = 8$). Finally, for an extremely elastic cell phase ($\tilde{E} = 30$), or equivalently for a very low nuclear rigidity, the cellular aggregate can penetrate the thickest ECM region for all considered values of β_0. It is also worth noting that as the value of β_0 increases the velocity of the aggregate expansion decreases.

As done for the single cell model, we here discuss the choices of the parameter values with respect to the biological data at the macroscopic scale. The literature based estimations of these parameters are collected in Table 2. The cell stress-free volume ratio and the contact inhibition volume ratio strongly depend on the tissue considered. From the range of the maximum ECM fiber volume fraction ($0.006 - 0.4$) and the maximum cell volume fraction ($0.4 - 0.85$) reported by Jain et al. [31], it is possible to estimate the contact inhibition volume ratio $0.406 \leq \psi_0 < 1$. Then, the stress-free volume ratio ϕ_n should be less than the cell volume fraction that triggers contact inhibition, i.e., $\phi_n < \psi_0 - \phi_m$. Thus, the values set in the simulations presented in Fig. 6 ($\phi_m = 0.15, 0.22$, $\psi_0 = 0.7$, $\phi_n = 0.45$) perfectly lie within the

Table 2 Biologically meaningful ranges for the parameters of the macroscopic model.

Parameter	Description	Values	Ref.
ϕ_n	stress-free volume ratio	$\phi_n < \psi_0 - \phi_m$	[–]
ψ_0	contact inibition threshold volume ratio	$0.406 - 1$	[31]
γ_c	cell duplication rate	$0.38 - 1.6$ days^{-1}	[8]
δ_c	cell apoptotic rate	~ 0.1 days^{-1}	[8]
α	motility parameter	$\sim 0.0051\ (\mathrm{Pa}\cdot\mathrm{s})^{-1}$	See text
E	cell aggregate Young's Modulus	$130 - 5000$ Pa	[46]
A_f	area of fibre bundle cross-section	$0.78 - 132$ μm^2	[36, 55]

biological range.
The motility parameter α can be estimated from eq. (24), equating the motility M to the permeability K and considering $n = 0$. By assuming fiber bundles with circular cross-section and radius equal to 1 μm [36, 55] and considering $\phi_m = 0.2$, the inversion of eq. (25) leads to $A_m \simeq 20$ μm^2. In [70], it is reported that isolated cells can migrate across pores with dimension equal to 10% of the original nucleus cross-section, so referring to the range of values of R_n reported in Table 1, we infer $A_0 = 0.71 - 7.85$ μm^2. Finally, in accordance with the estimation of the permeability $K \simeq 10^{-13}\mathrm{m}^2\ (\mathrm{Pa}\cdot\mathrm{s})^{-1}$ [45], we obtain $\alpha \simeq 0.005 - 0.008(\mathrm{Pa}\cdot\mathrm{s})^{-1}$. The Young's modulus of the cell phase reported in [46] shows a wide variance depending on the considered tissue (for normal mammary gland E lies in the range $130 - 200$ Pa, whereas for an average tumor it lies in the range $3000 - 5000$ Pa). The biological measurement of the aggregate Young's modulus combined with the shear modulus of the cell nucleus (see Table 1) gives a range for $\tilde{E}$ ($\approx 0.0012 - 71.5$) that perfectly includes the range set in the numerical simulations in Fig. 6.

5 Discussion and Conclusions

This work moves a step towards the definition of a theoretical and numerical tool able to analyze the role of nuclear stiffness along with cell active-adhesive abilities and stress condition on the migratory process of single cells and multicellular spheroids inside three dimensional extracellular environments. Treating the nucleus as an elastic solid surrounded by an elastic membrane, we identified an energy-based criterium for cells' ability to squeeze inside constrictions in 3D ECM. The criterium is given both in the case of a single cell entering inside a cylindrical channel and in the case of a multicellular aggregates moving inside a regular extracellular environment.

The energy balance criterium leads to the definition of the dimensionless numbers G_μ and $G_{passive}$, which represent the ratios between either active-adhesive properties of the cell, when the nucleus is actively pulled inside the channel (as in the single cell case), or a measure of the passive stress exerted on the cell, when the nucleus is forced inside the surrounding environment (for instance, when cells at the border of a multicellular aggregate are pushed by growth through the ECM surrounding it),

and the mechanical properties of the nuclear interior. At the cell scale, the model provides the relation that these characteristic numbers should satisfy in order to have cells entering a channel of a given radius, during MMP-inhibited migration, depending on the size of the nucleus and the ratio of the mechanical properties of the nuclear membrane over the ones of the inner solid material. Therefore, knowing either the active (i.e., the capability of the cell to express adhesion molecules and to actively generate sufficiently strong traction forces) or passive forces acting on the cell and the geometrical (i.e., the size) and mechanical (i.e., the stiffness) properties of the cell nucleus, it is possible to derive the minimum channel size that can be penetrated by the cell. Furthermore, by embedding the energy criterium inside the equations that describe the macroscopic evolution of a multicellular aggregate, it is possible to numerically simulate situations in which cell aggregates and growing tumors, in the absence of MMP secretion, can be compartmentalized by the surrounding thick extracellular matrix with a sufficiently low pore dimension. Thus, this work proves that nuclear stiffness and nuclear envelope stretchability, along with ECM microstructure, play an important role in cells' migration inside 3D environments and it shows that a too stiff nucleus or a non-stretchable nuclear membrane would nullify any attempt of the cell to squeeze through channels and network gaps narrower than the nucleus dimension, both in the case of single cell and multicellular invasion, in accordance with biological experiments [11,51,70,71]. Indeed, reduced levels of the nuclear envelope proteins lamins A/C, which is one of the determinants of nuclear stiffness, results in significantly faster passage of a cell through narrow constrictions during active and passive migration [11]. Furthermore, given the recent biological finding [30] that a variety of human cancers have altered lamin expression, the proposed model could be a useful tool in studying how changes in nuclear stiffness and stretchability, related to alterations in nuclear body's and envelope's structure and composition, may limit tumor invasion and metastasis formation, promoting the compartmentalization of cancer cell invasion or slowing down their migration through dense tissues or other confined spaces.

However, the model has been derived under some simplifications, that can possibly be dropped. At the macroscopic scale, the passive criterium obtained for multicellular aggregate motion should be extended in order to incorporate the active response of cells to stress and external stimuli. At the cell scale, it would be important to consider the dynamics of cell migration, including all the steps of the deformation and of the active force generation processes, possibly considering more complex geometries of the deformed nucleus (e.g., hourglass deformed nucleus [70]), the ECM response to stress and eventually more realistic constitutive laws representing the cytoplasm and nucleus. In particular, the model is derived assuming incompressibility of the nuclear material, in accordance with [37, 63], whereas the nuclear Poisson's ratio may vary between 0.3-0.5 [62]. Thus, future development of the model should consider the compressibility of the nuclear component. Instead, considering the viscous behavior of the cell nucleus [10, 12, 26], given the typical time scales required for deformation and relaxation, will not provide a real breakthrough in the present research.

Finally, the active-adhesive abilities of the cell, as well as its mechanical properties, can be possibly related to the mechanisms occurring at the smaller scale, such as the expression and activation of integrins, the cytoskeletal mechanics, the chromatin

mechanical response and the expression of lamins in the nuclear lamina, possibly supported by biological tests. In particular, elucidation of the mechanisms by which adhesions form and disassemble in time and space, possibly considering integrins' clustering and their non-homogeneous distribution inside the cell membrane [9, 67], might give a deeper insight on the whole dynamic phenomenon. Furthermore it was experimentally observed the existence, at the microscopic scale, of a critical ligand density (i.e., critical inter-ligand spacing) essential for stable assembly of focal adhesions [7, 44] and a minimum area of integrin-ligand clusters required for active force generation [9]. These thresholds are not constant, but they dynamically evolve, resulting from an equilibrium between pathways controlling adhesive force, cytoskeletal tension, and the structural linkage that transmits these forces [9]. Finally, it was recently observed that the relation between the force generated and the dimension of the focal adhesion region is neither constant nor linear [9], thus future work should consider the non-linear relation between the active traction force and the adhesive region estimated from experiments.

In spite of all possible developments, the energetic framework presented in this work is able to estimate the critical value of the pore size representing the "physical limit of migration" [70] that can be used in tumor growth models to predict their evolution and invasive potential in thick regions of ECM. In this respect, the proposed model might foster our understanding on pharmacological or biological approaches that can reduce tumor metastatic capabilities by inhibiting nuclear deformation and altering the transmigration of cancer cells.

References

1. A. Arduino, L. Preziosi. *A multiphase model of tumour segregation in situ by a heterogeneous extracellular matrix*. Int. J. Nonlinear Mech. 75: 22 – 30 (2015).
2. E.M. Balzer, Z. Tong, C.D. Paul, W.C. Hung, K.M. Stroka, A.E. Boggs, S.S. Martin, K. Konstantopoulos. *Physical confinement alters tumor cell adhesion and migration phenotypes.* FASEB J. 26(10):4045 – 4056 (2012).
3. C. Beadle, M.C. Assanah, P. Monzo, R. Vallee, S.S. Rosenfeld, P. Canoll. *The role of myosin II in glioma invasion of the brain*. Mol. Biol. Cell. 19: 3357 – 3368 (2008).
4. D.E. Birk, R.L. Trelstad. *Extracellular compartments in matrix morphogenesis: collagen fibril, bundle, and lamellar formation by corneal fibroblast.* J. Cell Biol. 99: 2024 – 2033 (1984).
5. V. te Boekhorst, L. Preziosi, P. Friedl. *Plastiticy of cell migration in vivo and in silico.* Annu. Rev. Cell Dev. Biol. 32: 491 – 526 (2016).
6. J.L. Broers, E.A. Peeters, H.J. Kuijpers, J. Endert, C.V. Bouten, C.W. Oomens, F.P. Baaijens, F.C. Ramaekers. *Decreased mechanical stiffness in LMNA-/-cells is caused by defective nucleo-cytoskeletal integrity: implications for the development of laminopathies.* Hum. Mol. Genet. 13: 2567 – 2580 (2004).
7. E.A. Cavalcanti-Adam, T. Volberg, A. Micoulet, H. Kessler, B. Geiger and J.P. Spatz. *Cell Spreading and Focal Adhesion Dynamics Are Regulated by Spacing of Integrin Ligands.* Biophys. J. 92: 2964 – 2974 (2007).
8. M.A.J. Chaplain, L. Graziano, L. Preziosi. *Mathematical modelling of the loss of tissue compression responsiveness and its role in solid tumour development.* Math. Med. Biol. 23: 197 – 229 (2006).
9. S.R. Coyer, A. Singh, D.W. Dumbauld, D.A. Calderwood, S.W. Craig, E. Delamarche, A.J. García. *Nanopatterning reveals an ECM area threshold for focal adhesion assembly and force transmission that is regulated by integrin activation and cytoskeleton tension.* J. Cell. Sci. 125 (Pt 21): 5110 – 5123 (2012).
10. K.N. Dahl, S.M. Kahn, K.L. Wilson and D.E. Discher. *The nuclear envelope lamina network has elasticity and a compressibility limit suggestive of a molecular shock absorber.* J. Cell Sci. 117: 4779 – 4786 (2004).

11. P.M. Davidson, C. Denais, M.C. Bakshi, J. Lammerding *Nuclear deformability constitutes a rate-limiting step during cell migration in 3-D environments*. Cell. Mol. Bioeng. 7(3): 293 – 306 (2014).
12. S. Deguchi, M. Yano, K. Hashimoto, H. Fukamachi, S. Washio, K. Tsujioka. *Assessment of the mechanical properties of the nucleus inside a spherical endothelial cell based on microtensile testing.* J. Mech. Mater. Struct. 2(6): 1087 – 1102 (2007).
13. E.A. Evans, R. Waugh, L. Melnik *Elastic area compressibility modulus of red cell membrane.* Biophys. J. 16: 585 – 595 (1976).
14. G.R. Fedorchak, A. Kaminski, J. Lammerding. *Cellular mechanosensing: getting to the nucleus of it all.* Prog. Biophys. Mol. Biol. 115: 76 – 92 (2014).
15. P. Friedl, E.B. Brocker. *The biology of cell locomotion within three-dimensional extracellular matrix*. Cell. Mol. Life Sci. 57 (1): 41 – 64 (2000).
16. P. Friedl, E. Sahai, S. Weiss, K.M. Yamada. *New dimensions in cell migration.* Nat. Rev. Mol. Cell Biol. 13(11):743 – 747 (2012).
17. P. Friedl, K. Wolf. *Tumour-cell invasion and migration: diversity and escape mechanisms*. Nat. Rev. Cancer. 3 (5): 362 – 374 (2003).
18. P. Friedl, K. Wolf. *Plasticity of cell migration: a multiscale tuning model.* J. Cell Biol. 188(1): 11 – 19 (2010).
19. P. Friedl, K, Wolf, J. Lammerding. *Nuclear mechanics during cell migration*. Curr. Opin. Cell. Biol. 23 (1): 55 – 64 (2011).
20. Y. Fu, L.K. Chin, T. Bourouina, A.Q. Liu, A.M. VanDongen. *Nuclear deformation during breast cancer cell transmigration.* Lab Chip. 12(19): 3774 – 3778 (2012).
21. G. Gerlitz, M. Bustin. *The role of chromatin structure in cell migration*. Trends Cell. Biol. 21 (1): 6 – 11 (2011).
22. C. Giverso C, A. Grillo, L. Preziosi. *Influence of nucleus deformability on cell entry into cylindrical structures*. Biomech. Model Mechanobiol. 13(3): 481 – 502 (2014).
23. C. Giverso, M. Scianna, A. Grillo. *Growing avascular tumours as elasto-plastic bodies by the theory of evolving natural configurations.* Mech. Re. Commun. 68: 31 – 39 (2015).
24. F. Graner, J. A. Glazier. *Simulation of biological cell sorting using a two-dimensional extended potts model*. Phys. Rev. Let. 69: 2013 – 2016 (1992).
25. J. Guck, F. Lautenschläger, S. Paschke, M. Beil. *Critical review: cellular mechanobiology and amoeboid migration*. Integr. Biol. 2: 575 – 583 (2010).
26. F. Guilak, J.R. Tedrow, and R. Burgkart. *Viscoelastic Properties of the Cell Nucleus.* Biochem. Biophys. Res. Commun. 269, 781 – 786 (2000).
27. H. Liu, J. Wen, Y. Xiao, J. Liu, S. Hopyan, M. Radisic, C.A. Simmons, and Y. Sun. *In Situ Mechanical Characterization of the Cell Nucleus by Atomic Force Microscopy.* ACS Nano 8(4): 3821 – 3828 (2014).
28. T. Harada, J. Swift, J. Irianto, J.W. Shin, K.R. Spinler, A. Athirasala, R. Diegmiller, P.C. Dingal, I.L. Ivanovska, D.E. Discher. *Nuclear lamin stiffness is a barrier to 3D migration, but softness can limit survival.* J. Cell. Biol. 204: 669 – 682 (2014).
29. W. Helfrick. *Elastic properties of lipid bilayers: theory and possible experiments*. Z. Naturforsch. 28(11): 693 – 703 (1973).
30. C.Y. Ho, J. Lammerding. *Lamins at a glance.* J. Cell Sci. 125(Pt 9): 2087 – 2093 (2012).
31. R.K. Jain. *Transport of Molecules in the Tumor Interstitium: A Review.* Cancer Res. 47: 3039 – 3051 (1987).
32. W.C. Hung, S.H.Chen, C.D. Paul, K.M. Stroka, Y.C. Lo, J.T. Yang, K. Konstantopoulos. *Distinct signaling mechanisms regulate migration in unconfined versus confined spaces.* J. Cell Biol. 202(5): 807 – 824 (2013).
33. P. Isermann, J. Lammerding. *Nuclear Mechanics and Mechanotransduction in Health and Disease*. Curr. Biol. 23(24): R1113 – R1121 (2013).
34. A. Kaufmann, F. Heinemann, M. Radmacher, R. Stick. *Amphibian oocyte nuclei expressing lamin A with the progeria mutation E145K exhibit an increased elastic modulus.* Nucleus 2: 310 – 319 (2011).
35. M-C Kim, D.M. Neal, R.D. Kamm, H.H. Asada. *Dynamic modeling of cell migration and spreading behaviors on fibronectin coated planar substrates and micropatterned geometries.* PLoS Comput. Biol. 9(2): e1002926 (2013).
36. Y. Komai, T. Ushiki. *Three-dimensional organization of collagen fibrils in the human cornea and sclera.* Investig. Ophthalmol. Vis. Sci. 32(8): 2244 – 2258 (1991).
37. M. Krause, J. Te Riet, K. Wolf. *Probing the compressibility of tumor cell nuclei by combined atomic force-confocal microscopy.* Phys. Biol. 10(6): 065002 (2013).

38. M. Krause, K. Wolf *Cancer cell migration in 3D tissue: Negotiating space by proteolysis and nuclear deformability.* Cell Adhes. Migr. 9(5): 357 – 366 (2015).
39. J. Lammerding, L.G. Fong, J.Y. Ji, K. Reue, C.L. Stewart, S.G. Young, R.T. Lee. *Lamins A and C but not lamin B1 regulate nuclear mechanics.* J. Biol. Chem. 281: 25768 – 25780 (2006).
40. F. Lautenschläger, S. Paschke, S. Schinkinger, A. Bruel, M. Beil, J. Guck. *The regulatory role of cell mechanics for migration of differentiating myeloid cells*. PNAS 106 (37): 15696 – 15701 (2009).
41. M.L. Lombardi, L. Lammerding. *Keeping the LINC: the importance of nucleocytoskeletal coupling in intracellular force transmission and cellular function.* Biochem. Soc. Trans. 39: 1729 – 1734 (2011).
42. J.S Lowengrub, H.B Frieboes, F. Jin, Y.L Chuang, X. Li, P. Macklin, S.M. Wise, V. Cristini. *Nonlinear modelling of cancer: bridging the gap between cells and tumours*. Nonlinearity. 23: R1 – R91 (2010).
43. E. Makhija, D.S. Jokhun, G.V. Shivashankar. *Nuclear deformability and telomere dynamics are regulated by cell geometric constraints.* PNAS 13(1): E32 – E40 (2015).
44. S.P. Massia and J.A. Hubbell. *An RGD spacing of 440 nm is sufficient for integrin $\alpha_v - \beta_3$-mediated fibroblast spreading and 140 nm for focal contact and stress fiber formation.* J. Cell Biol. 114 (5): 1089 – 1100 (1991).
45. P.A. Netti, R.K. Jain. *Interstitial transport in solid tumours.* in **Cancer Modelling and Simulation**, L. Preziosi, Ed., CRC-Press - Chapman Hall, Boca Raton (2003).
46. M.J. Paszek, et al. *Tensional homeostasis and the malignant phenotype.* Cancer Cell. 8: 241 – 254 (2005).
47. R.J. Petrie, K.M. Yamada. *At the leading edge of three-dimensional cell migration.* J. Cell Sci. 125(Pt 24): 5917 – 5926 (2012).
48. L. Preziosi, A. Tosin. *Multiphase and multiscale trends in cancer modelling*. Math. Model. Nat. Phenom. 4(3): 1 – 11 (2009).
49. P. Rajagopalan, W.A. Marganski, X.Q. Brown, J.Y. Wong. *Direct comparison of the spread area, contractility, and migration of balb/c 3T3 fibroblasts adhered to fibronectin- and RGD-modified substrata.* Biophys. J. 87(4): 2818 – 2827 (2004).
50. A.J. Ribeiro, P. Khanna, A. Sukumar, C. Dong, K.N. Dahl. *Nuclear stiffening inhibits migration of invasive melanoma cells.* Cell Mol. Bioeng. 7(4): 544 – 551 (2014).
51. C.G. Rolli, T. Seufferlein, R. Kemkemer, J.P. Spatz. *Impact of tumor cell cytoskeleton organization on invasiveness and migration: A microchannel-based approach.* PLos ONE. 5 (1): e8726 (2010).
52. A.C. Rowat, J. Lammerding, H. Herrmann, U. Aebi. *Towards an integrated understanding of the structure and mechanics of the cell nucleus.* BioEssays 30: 226 – 236 (2008).
53. F. Sabeh, R. Shimizu-Hirota, S.J. Weiss. *Protease-dependent versus -independent cancer cell invasion programs: three-dimensional amoeboid movement revisited*. J. Cell. Biol. 185 (1): 11 – 19 (2009).
54. E. Sahai. *Illuminating the metastatic process*. Nat. Rev. Cancer. 7 (10): 737 – 749 (2007).
55. I.S. Saidi, S.L. Jacques, F.K. Tittel. *Mie and Rayleigh modeling of visible-light scattering in neonatal skin.* Appl. Opt. 34(31): 7410 – 7418 (1995).
56. M. Schoumacher, R.D. Goldman, D. Louvard, and D.M. Vignjevic. *Actin, microtubules, and vimentin intermediate filaments cooperate for elongation of invadopodia.* J. Cell Biol. 189: 541 – 556 (2010).
57. J. Shankar, A. Messenberg, J. Chan, T.M. Underhill, L.J. Foster, and I.R. Nabi. *Pseudopodial actin dynamics control epithelial-mesenchymal transition in metastatic cancer cells.* Cancer Res. 70: 3780 – 3790 (2010).
58. L.M. Shaw. *Tumor Cell Invasion Assays*. In: Cell Migration: Developmental Methods and Protocols vol. 294, J-L Guan Ed., Humana Press: 97 – 105 (2005).
59. R. Skalak, A. Tozeren, R.P. Zarda, S. Chien. *Strain energy function of red blood cell membrane*. Biophys. J. 13: 245 – 264 (1973).
60. Z.C. Tu, Z.C. Ou-Yang. *Geometric theory on the elasticity of bio-membranes*. J. Phys. A: Math. Gen. 37: 11407 – 11429 (2004).
61. Z.C. Tu, Z.C. Ou-Yang. *Elastic theory of low-dimensional continua and its applications in bio- and nano-structures*. J. Comput. Theor. Nanosci. 5: 422 – 448 (2008).
62. R. Vargas-Pinto, H. Gong, A. Vahabikashi and M. Johnson. *The effect of the endothelial cell cortex on atomic force microscopy measurements.* Biophys. J. 105: 300 – 309 (2013).
63. A. Vaziri, H. Lee, and M.R. Kaazempur Mofrad, *Deformation of the cell nucleus under indentation: mechanics and mechanisms.* J. Mater. Res. 21: 2126 – 2135 (2006).
64. C. Verdier, J. Etienne, A. Duperray, L. Preziosi. *Review: Rheological properties of biological materials*. C. R. Phys. 10(8): 790 – 811 (2009).
65. M. Versaevel, T. Grevesse, S. Gabriele. *Spatial coordination between cell and nuclear shape within micropatterned endothelial cells*. Nature Comm. 3: 671 (2012).

66. B. Weigelin, G-J. Bakker, P. Friedl. *Intravital third harmonic generation microscopy of collective melanoma cell invasion. Principles of interface guidance and microvesicle dynamics.* IntraVital. 1(1): 32 – 43 (2012).
67. P.W. Wiseman, C.M. Brown, D.J. Webb, B. Hebert, N.L. Johnson, J.A. Squier, M.H. Ellisman and A.F. Horwitz. *Spatial mapping of integrin interactions and dynamics during cell migration by Image Correlation Microscopy.* J. Cell. Sci. 117: 5521 – 5534 (2004).
68. K. Wolf, S. Alexander, V. Schacht, L.M Coussens, U.H von Andrian, J. van Rheenen, E. Deryugina, P. Friedl. *Collagen-based cell migration models in vitro and in vivo*. Semin. Cell. Dev. Biol. 20 (8): 931 – 941 (2009).
69. K. Wolf, P. Friedl. *Extracellular matrix determinants of proteolytic and non-proteolytic cell migration*. Trends. Cell. Biol. 21 (12): 736 – 744 (2011).
70. K. Wolf, M. Te Lindert, M. Krause, S. Alexander, J. Te Riet, A.L. Willis, R.M. Hoffman, C.G. Figdor, S.J. Weiss, P. Friedl. *Physical limits of cell migration: control by ECM space and nuclear deformation and tuning by proteolysis and traction force.* J. Cell Biol. 201(7): 1069 – 1084 (2013).
71. K. Wolf, Y.I. Wu, Y. Liu, J. Geiger, E. Tam, C. Overall, M.S. Stack, P. Friedl. *Multi-step pericellular proteolysis controls the transition from individual to collective cancer cell invasion*. Nat. Cell. Biol. 9: 893 – 904 (2007).